European Journal of Nutrition (2024) 63:1929–1944
https://doi.org/10.1007/s00394-024-03401-2

ORIGINAL CONTRIBUTION

Improvement of functional dyspepsia with *Suaeda salsa* (L.) Pall via regulating brain-gut peptide and gut microbiota structure

Wenjun Zhang[1] · Xueyu Wang[1] · Shuanghui Yin[1] · Ye Wang[1] · Yong Li[1] · Yuling Ding[1]

Received: 19 January 2024 / Accepted: 10 April 2024 / Published online: 4 May 2024

Abstract

Purpose The traditional Chinese herbal medicine *Suaeda salsa* (L.) Pall (*S. salsa*) with a digesting food effect was taken as the research object, and its chemical composition and action mechanism were explored.

Methods The chemical constituents of *S. salsa* were isolated and purified by column chromatography, and their structures were characterized by nuclear magnetic resonance. The food accumulation model in mice was established, and the changes of the aqueous extract of *S. salsa* in gastric emptying and intestinal propulsion rate, colonic tissue lesions, serum brain-gut peptide hormone, colonic tissue protein expression, and gut microbiota structure were compared.

Results Ten compounds were isolated from *S. salsa* named as naringenin (**1**), hesperetin (**2**), baicalein (**3**), luteolin (**4**), isorhamnetin (**5**), taxifolin (**6**), isorhamnetin-3-*O*-β-D-glucoside (**7**), luteolin-3′-D-glucuronide (**8**), luteolin-7-*O*-β-D-glucuronide (**9**), and quercetin-3-*O*-β-D-glucuronide (**10**), respectively. The aqueous extract of *S. salsa* can improve the pathological changes of the mice colon and intestinal peristalsis by increasing the rate of gastric emptying and intestinal propulsion. By adjusting the levels of 5-HT, CCK, NT, SS, VIP, GT-17, CHE, MTL, and ghrelin, it can upregulate the levels of c-kit, SCF, and GHRL protein, and restore the imbalanced structure of gut microbiota, further achieve the purpose of treating the syndrome of indigestion. The effect is better with the increase of dose.

Conclusion *S. salsa* has a certain therapeutic effect on mice with the syndrome of indigestion. From the perspective of "brain-gut-gut microbiota", the mechanism of digestion and accumulation of *S. salsa* was discussed for the first time, which provided an experimental basis for further exploring the material basis of *S. salsa*.

Keywords *Suaeda salsa* (L.) Pall · Functional dyspepsia · Gastrointestinal hormone · Brain-gut peptide · Gut microbiota

Introduction

Functional dyspepsia (FD), often referred to as "Shi Ji", in traditional Chinese medicine is largely due to irrational eating behaviors and subsequent food retention in the gastrointestinal tract, thus affecting digestive function [1]. Nowadays, people consume more calories and more people suffer from digestive disorders which gradually leads to a higher incidence of metabolic diseases [2]. In FD, unlike organic dyspepsia, there is no underlying organic disease that can cause symptoms of dyspepsia. Changes in immune and mucosal functions, gastric motility disorders, brain-gut axis interactions, different compositions of the gastrointestinal microbiota, and changes in central nervous system processing are considered to be the causes of FD, and gastrointestinal motility disorders are the main clinical manifestations [3, 4].

The brain-gut axis is a conceptual model of a two-way connection between the gut and the central nervous system [5]. The two interact with each other, also known as "brain-gut interaction". Besides the interaction of the central nervous system, autonomic nervous system, and intestinal nervous system, the regulation of the nervous system on the gastrointestinal tract also includes the hypothalamus–pituitary–adrenal (HPA) axis. Among them, the HPA axis determines the receptors of intestinal physiological activities and plays an important role in regulating gastrointestinal dysfunction [5]. Brain-gut peptide is a peptide

Wenjun Zhang and Xueyu Wang have contributed equally to this work.

✉ Yuling Ding
dingyl@ccucm.edu.cn

[1] School of Pharmaceutical Sciences, Changchun University of Chinese Medicine, Changchun 130117, Jilin, China

distributed in the brain and gastrointestinal tract. It is an important regulatory factor and participates in the regulation of gastrointestinal physiological activities [6]. Studies have confirmed that brain-gut peptide can improve gastrointestinal motility disorders by regulating gastric emptying and intestinal propulsion and has a significant effect on the treatment of FD [7]. The gastrointestinal tract is a whole, and the intestinal microbiome is located in the intestinal cavity. The stability of the intestinal microbiota is also the key factor to ensure the normal function of the gastrointestinal tract. Studies have confirmed that by regulating the structure of intestinal microbiota, gastrointestinal dysfunction can be improved following by FD improvement [8]. Intestinal microorganisms can also change brain structure and function through endocrine, neural, and inflammatory signals, while autonomic nervous system activities can affect the microbiome by regulating the intestinal environment and directly regulating microbial behavior [9]. Therefore, the concept of "brain-gut-gut microbiota axis" appears, and the three jointly affect gastrointestinal health [10].

Suaeda salsa (L.) Pall (*S. salsa*) is an annual herb that belongs to the *Chenopodiaceae* family. In the northern coastal areas of China, people usually pick its seedlings for cooking. According to the Chinese classic masterpiece of *Ben Cao Gang Mu Shi Yi*, *S. salsa* has the effect of clearing away heat and dissipating food accumulation, mainly treating for indigested syndrome with epigastric [11], but its mechanism has not been systematically evaluated. According to Traditional Chinese Medicine (TCM) dialectics, there are two common causes of food accumulation: one is dyspepsia due to improper feeding, and the other is syndrome of malnutrition due to spleen deficiency. Usually, the treatment for dyspepsia due to improper feeding is through promoting digestion and relieving dyspepsia. Therefore, the digest food and dissipate the food accumulation effect of *S. salsa* mainly targets the indigested syndrome with epigastric caused by dyspepsia due to improper feeding. With the high pressure of people's lives, overeating, and eating too greasy and indigestible food can easily lead to dyspepsia due to improper feeding, which leads to food accumulation, that is, diet stagnation FD. According to the previous research report of our experimental team, according to the chemical classification of natural products, the chemical components of *S. salsa* occupy almost all categories, most of which are flavonoids [12]. Flavonoids exist in most fruits and foods for daily drinking, and have beneficial effects on the regulation of gastrointestinal function, the metabolism of intestinal microbiota, and the maintenance of gastrointestinal health [13]. More and more literatures have reported that common flavonoids can regulate the structural changes of intestinal microbiota caused by a high-fat diet and improve FD [14–16].

Therefore, this experiment fed mice with a high-fat diet to create dyspepsia due to the improper feeding model of mice. By observing the effect of *S. salsa* extract on the FD model mice to explore its mechanism from the regulation of brain-gut-gut microbial axis homeostasis, this experiment provides an experimental basis for the clinical application and product development of *S. salsa*.

Materials and methods

Materials

S. salsa was collected from near Red Beach, Panjin City, Liaoning Province, China. It was identified by Professor Zhang Jinglong, School of Pharmaceutical Sciences, Changchun University of Chinese Medicine as *Suaeda salsa* (L.) Pall. The specimens of *S. salsa* medicinal materials were preserved in the Herbarium of Changchun University of Chinese Medicine, China (No. A50337120210826YDJP). The rest of the medicinal herbs removed impurities such as sediment took the aboveground part, and cut the section for later use. 5-hydroxytryptamine (5-HT) ELISA kit (MM-0443M1), cholecystokinin (CCK) ELISA kit (MM-0028M1), neurotensin (NT) ELISA kit (MM-463554M1), somatostatin (SS) ELISA kit (MM-0493M1), vasoactive intestinal peptide (VIP) ELISA kit (MM-0446M1), gastrin-17 (GT-17) ELISA kit (MM-46046M1), cholinesterase (CHE) ELISA kit (MM-0920M1), motilin (MTL) ELISA kit (MM-0492M1), and ghrelin ELISA kit (MM-0621M1) were purchased from Jiangsu Meimian Industrial Co., Ltd, China. BCA protein concentration determination kit was purchased from Beijing Solarbio Science & Technology Co., Ltd, China. C-Kit Antibody (AF6153##1278) was purchased from Jiangsu Qinke Biological Research Center Co., Ltd, China. SCF Antibody (26582-1-AP), GHRL Polyclonal Antibody (13309-1-AP), GAPDH Antibody (10494-1-AP), and HRP-conjugated Affinipure Goat Anti-Rabbit lgG (H + L) (SA00001-2) were purchased from Wuhan Sanying Biotechnology Co., Ltd, China. SuperSignal™ West Femto kit (34094) was purchased from Thermo Fisher Scientific, USA.

Extraction and separation

Took 171 kg of dry *S. salsa* stems and branches, added 10 times of water, soaked for 30 min, decocted for 30 min, and filtered. Added 8 times of water to the filter residue, decocted for 20 min, and filtered. Combined the two filtrates and concentrated them to a certain volume ($\rho = 1.22$). While stirring the liquid at a constant speed

with an agitator, slowly poured anhydrous ethanol at a constant speed until the ethanol concentration reached to 65%. Sealed and placed in a cool place for 12 h. Filtered to remove polysaccharide, collected filtrate, and concentrated to extract.

The extract was desalted with 200 g HP-20 macropore resin, and the column were flushed with five column volumes of distilled water to remove salt, followed with 4 column volumes of methanol, after recovering methanol, the crude extract (940 g) was obtained. The extract was dissolved in water and then extracted with petroleum ether, chloroform, ethyl acetate, and water-saturated *n*-butanol by gradient-polarity solvent extraction method at the extraction ratio of 1:1 (*V*/*V*), and the extraction was performed three times. The extracted liquid was combined and the organic solvent of each chemical part was recovered with a rotary evaporator to obtain four chemical parts, namely Fr.PE (69.4 g), Fr.CH (47.1 g), Fr.EA (121.3 g), and Fr.Bu (37.5 g), stored at 4℃ for standby.

Took Fr.EA (121.3 g), wet silica gel column-packing, eluting with *n*-hexane/EtOAc (10:0–0:10), EtOAc/MeOH (20:0–0:20). The eluent was collected with a 30 ml test tube, and each tube was checked by TLC. The tubes with the same target were combined and concentrated, and a total of 8 sub-fractions Fr.EA-1–8 were obtained. Fr.EA-4 was isolated by silica gel column chromatography, and chloroform/MeOH (10:0–0:10) was used as eluent to obtain Fr.EA-4A–4E. Fr.EA-4A was purified by Sephadex LH-20 column, and chloroform/MeOH (1:1) was used as eluent to obtain compound **1** (69.3 mg), compound **2** (54.4 mg), and compound **5** (87.9 mg). Fr.EA-4B and Fr.EA-4C were purified by silica gel column chromatography with chloroform/MeOH (10:0–0:10) to obtain compound **3** (32.1 mg), compound **4** (10.4 mg), and compound **6** (11.6 mg). Fr.EA-8 was purified by silica gel column chromatography and eluted with EtOAc/MeOH (10:0–0:10) to obtain compound **7** (7.9 mg).

Took Fr.Bu (37.5 g) and dried silica gel column-packing. The mobile phase was chloroform/MeOH (15:0–0:15) gradient elution, and six sub-fractions of Fr.Bu-1–6 were obtained. Fr.Bu-2 was eluted with ethanol–water (0, 10%, 20%, 40%, 60%, 80%, 100%) by macropore resin column chromatography, and a total of seven components of Fr.Bu-2A–2G were obtained. Fr.Bu-2C was eluted with ethanol–water (0, 10%, 20%, 40%, 60%, 80%, 100%) by macropore resin column chromatography to obtain Fr.Bu-2C.1–2C.7. Fr.Bu-2C.3 was purified by a silica gel column, and EtOAc/MeOH (10:0–0:10) was used as eluent to obtain compound **8** (21.8 mg). Fr.Bu-2C.4 was chromatographed on the Sephadex LH-20 column and eluted with methanol–water (0, 10%, 20%, 40%, 60%, 80%, 100%), compound **9** (55.6 mg) and compound **10** (20.7 mg) were obtained in 40% mobile phase.

Preparation of crude extract of *S. salsa*

Took 2 kg of dry *S. salsa* stems and branches, added 10 times the amount of water to soak for 30 min, and decocted for 30 min. After filtering, added 8 times the amount of water, decocted again for 20 min, and filtered. The crude extract was obtained. Took 5 g, 10 g, and 20 g of the extract respectively, and added 50 ml of water to dissolve them to prepare 0.1 g/ml, 0.2 g/ml, and 0.4 g/ml of the tested samples.

Animal

Specific Pathogen Free (SPF) grade male Kunming (KM) mice (3–4 weeks old, weighing 16–18 g) were purchased from Liaoning Changsheng Biotechnology Co., Ltd, China (Animal license number: SYXK (Liao) 2020-0001). Mice maintenance feed was purchased from Beijing Keao Xieli Feed Co., Ltd, China. Healthy male KM mice were maintained in a temperature-controlled room (22 ± 1°C) with a 12 h light/dark cycle and free access to normal chow and water. Animals were adapted to the environment for 1 week before starting the experiment.

FD model establishment

The mice were randomly divided into control group (CON group), model group (MOD group), positive drug group (DPLT and JWXSP group) and *S. salsa* crude extract group (low/medium/high dose group), with 8 mice in each group. The mice in the CON group were fed with normal fodder and gavaged with distilled water 20 ml/kg day The other groups were fed with a high-fat diet (soybean powder (g): meat floss (g): bread powder (g): milk powder (g) = 2:1:1, mixed with water, made into cookies, put into the bake oven, and dried at 36℃), and fed with 50% milk 20 ml/kg day to induce FD. After 10 days, the domperidone group and Jianwei Xiaoshi tablet group were given domperidone suspension of 6.15 mg/kg day and Jianwei Xiaoshi tablet suspension of 1474 mg/kg day respectively for 1 week. The low-dose group, middle-dose group, and high-dose group were given 0.1 g/ml day, 0.2 g/ml day, and 0.4 g/ml day of *S. salsa* crude extract respectively.

Observation of animal indicators

During the experiment, the food intake, stool excretion, stool morphology, and mental state of mice in each group were observed.

Sample collection

On the 24th day of the experiment, mice were fasted for 24 h after gavage. On the morning of the 25th day, mice in each group were given 0.4 ml nutritional semi-solid paste (sodium carboxymethyl cellulose 20 g, dry skimmed milk powder 16 g, starch 8 g, sucrose 8 g, activated carbon 2 g heated to make 500 ml semi-solid paste) by gavage for 1 h. After 20 min, the mice were anesthetized by intraperitoneal injection of 1% pentobarbital sodium (50–90 mg/kg). The blood was collected from the eyeballs of mice. The serum was collected by centrifugation at 4℃, and then frozen at −80°C. The anesthetized mice were sacrificed by cervical dislocation. The colon tissue was separated. Labeled the above tissues and stored them in the refrigerator at −80°C for standby.

Experiment of gastric emptying and intestinal propulsion

After the mice were sacrificed by cervical dislocation, the tissues of the stomach and small intestine were collected rapidly. The cardia and pylorus were ligated and the total and net weights of the stomach were weighed. Recorded the total length of the small intestine and the distance from the semisolid paste to the pylorus. The gastric emptying rate is calculated as Eq. (1), and the intestinal propulsion rate is calculated as Eq. (2). Equation (1): X is the mass of semi-solid paste; Y is the mass of gastric residue. Equation (2): A is the length of the small intestine of semi-solid paste; B is the total length of the small intestine.

$$\text{Gastric emptying } \% = (1 - X/Y) * 100 \quad (1)$$

$$\text{Intestinal propulsion } \% = A/B * 100 \quad (2)$$

Hematoxylin and eosin (H&E) staining

The colon tissues of mice were collected and fixed with paraformaldehyde solution for 24 h. Paraffin-embedded, sliced (slice thickness 3–4 μm), H&E staining. The pathological changes of colon tissue were observed under a microscope. Image Pro Plus 6.0 software was used for quantitative analysis of pathological changes of colon [17]. The histological score was graded as follows [18, 19]: (a) damage degree of intestinal mucosa (0 points = none, 1 points = base 1/3 damage, 2 points = base 2/3 damage, 3 points = completely damaged); (b): loss of intestinal villi (0 points = none, 1 points = mild, 2 points = moderate, 3 points = severe).

Enzyme-linked immunosorbent assay (ELISA)

The levels of 5-HT, CCK, NT, SS, VIP, GT-17, CHE, MTL, and ghrelin in 9 serums were detected by the ELISA kit. The experiment was carried out according to the manufacturer's instructions.

Western blot analysis

Took about 20 mg of mice colon tissue and added the corresponding volume of the lysate (add 10% for each 1 ml of lysate μl PMSF), ground it fully on ice, put it into a 4℃ centrifuge, centrifuged for 30 min at 12000r, took the supernatant and put it into a new EP tube and recorded the volume. A BCA protein concentration assay kit was used to determine the protein concentration. Medium amounts of proteins (30 μg) from the samples were separated and transferred to PVDF membranes using SDS-PAGE. 10% nonfat milk was used to block the membranes for 2 h and washed with Tris-buffered saline-T (TBST). This was followed by overnight incubation at 4°C with different primary antibodies to c-Kit (5:10000), SCF (10:10000), GHRL (1:1000), and GAPDH (2:10000, 10494-1-AP). After washing with 1× TBS containing 0.1% (*V/V*) Tween-20, incubated with secondary antibodies, respectively. Protein bands were detected with the SuperSignal™ West Femto kit and observed using a BLT Intelligent image Workstation (Gelview 6000Plus, Guangzhou Biolight Biotechnology Co., Ltd, China). The integrated optical density of the target protein was measured by ImageJ software, and the target protein was analyzed quantitatively.

Gut microbiota analysis

According to the instructions of the E.Z.N.A.® soil DNA kit (Omega Bio-tek, Norcross, GA, U.S.), the total DNA of the microbial community was extracted from the contents of mice cecum. 1% agarose gel electrophoresis was used to detect the quality of DNA extraction. The concentration and purity of DNA were determined by nanodrop2000. The V3-V4 region of 16S rRNA gene was amplified by PCR using 338F (5′-ACTCCTACGGGAGGCAGCAG-3′) and 806R (5′-GGACTACHVGGGTWTCTAAT-3′). After mixing the PCR products of the same sample, 2% agarose gel to recover the PCR products. The recovered product was purified by AxyPrep DNA Gel Extraction Kit (Axygen Biosciences, Union City, CA, USA), and detected by 2% agarose gel electrophoresis. Quantus™ Fluorometer (Promega, USA) detected and quantified the recovered products. Used NEXTFLEX Rapid DNA-Seq Kit to build the

database. The MiseqPE250 platform of Illumina Company was used for sequencing.

The index like Sobs, Ace, Chao, Shannon, Simpson, and Venn diagram were used to analyze species richness, diversity, and species composition through Uparse software platform. At the phylum level, R language (vegan) was used to analyze the community composition and the relationship between each group of samples and species. Based on the hierarchical clustering (hcluster) of the distance matrix, R language (vegan) is used for principal coordinate analysis. LEFSe used linear discriminant analysis (LDA) to estimate the impact of each species abundance on the difference effect, and identified the species with significant differences between groups. The effect size is 4.

Statistical analysis

The data were expressed as mean ± standard deviation (SD). Data processing was using GraphPad Prism 9, and multiple comparisons were evaluated using one-way analysis of variance (ANOVA). $P < 0.05$ results between groups were considered statistically as significance.

Results

Chemical structure identification

Ten compounds were isolated from the extracted layers of EtOAc and water-saturated *n*-butanol of *S. salsa* named as naringenin (**1**), hesperetin (**2**), baicalein (**3**), luteolin (**4**), isorhamnetin (**5**), taxifolin (**6**), isorhamnetin-3-*O*-β-D-glucoside (**7**), luteolin-3′-D-glucuronide (**8**), luteolin-7-*O*-β-D-glucuronide (**9**), quercetin-3-*O*-β-D-glucuronide (**10**) (Fig. 1).

Compound **1**: off-white powder. LR-EIMS: *m/z*, 272.256 ($C_{15}H_{12}O_5$). ^{1}H-NMR (400 MHz, MeOH-d_4, TMS), δ_H: 7.32 (2H, d, J = 8.6 Hz, H-2′, 6′), 6.83 (2H, d, J = 8.6 Hz, H-3′, 5′), 5.91 (1H, d, J = 2.2 Hz, H-8), 5.90 (2H, d, J = 2.2 Hz, H-6), 5.34 (1H, dd, J = 3.0 Hz, 13.0 Hz, H-2), 3.12 (1H, dd, J = 13.0 Hz, 17.1 Hz, H-3α), 2.70 (1H, dd, J = 3.0 Hz, 17.1 Hz, H-3β). ^{13}C-NMR (100 MHz, MeOH-d_4, TMS), δ_C: 196.4 (C-4), 167.0 (C-7), 164.1 (C-5), 163.5 (C-9), 147.6 (C-4′), 129.7 (C-1′), 127.7 (C-2′, 6′), 114.9 (C-3′, 5′), 102.0 (C-10), 95.6 (C-6), 94.8 (C-8), 79.1 (C-2), 42.6 (C-3). The data above were compared with those reported in the literature resulting in compound **1**, namely naringenin [20].

Compound **2**: beige yellow powder. LR-EIMS: *m/z*, 302.282 ($C_{16}H_{14}O_6$). ^{1}H-NMR (400 MHz, MeOH-d_4, TMS), δ_H: 6.97–6.91 (3H, m, H-2′, 5′, 6′), 5.92 (1H, d, J = 2.1 Hz, H-8) 5.90 (2H, d, J = 2.1 Hz, H-6), 5.33 (1H, dd, J = 3.1 Hz, 12.6 Hz, H-2), 3.88 (3H, s, H-7′), 3.08 (1H, dd, J = 12.6 Hz, 17.1 Hz, H-3α), 2.72 (1H, dd, J = 3.1 Hz, 17.1 Hz, H-3β). ^{13}C-NMR (100 MHz, MeOH-d_4, TMS), δ_C: 196.2 (C-4), 167.0 (C-7), 164.1 (C-5), 163.4 (C-9), 147.9 (C-4′), 146.4 (C-3′), 131.7 (C-1′), 117.6 (C-6′), 113.1 (C-2′), 111.2 (C-5′), 102.0 (C-10), 95.7 (C-6), 94.8 (C-8), 78.9 (C-2), 55.0 (C-7′), 42.7 (C-3). The data above were compared with those reported in the literature. So, compound **2** was identified as hesperetin [21].

Compound **3**: yellow powder. LR-EIMS: *m/z*, 270.24 ($C_{15}H_{10}O_5$). ^{1}H-NMR (400 MHz, DMSO-d_6, TMS), δ_H: 12.66 (1H, s, HO-5), 10.57 (1H, s, HO-7), 8.81 (1H, s, HO-6), 8.06 (2H, dd, J = 7.9 Hz, 1.5 Hz, H-2′, 6′), 7.63–7.55 (3H, m, H-3′, 4′, 5′), 6.93 (1H, s, H-8), 6.63 (1H, s, H-3). ^{13}C-NMR (100 MHz, DMSO-d_6, TMS), δ_C: 182.6 (C-4), 163.4 (C-2), 154.1 (C-7), 150.3 (C-9), 147.4 (C-5), 132.3 (C-4′), 131.4 (C-1′), 129.8 (C-6), 129.6 (C-3′, 5′), 126.8 (C-2′, 6′), 105.0 (C-3), 104.8 (C-10), 94.5 (C-8). The data above were compared with those reported in the literature resulting in compound **3**, namely baicalein [22].

Compound **4**: pale yellow powder. LR-EIMS: *m/z*, 286.23 ($C_{15}H_{10}O_6$). ^{1}H-NMR (400 MHz, MeOH-d_4, TMS), δ_H: 7.40–7.38 (2H, m, H-2′, 6′), 6.91 (1H, dd, J = 2.5 Hz, 8.9 Hz, H-5′), 6.54 (1H, s, H-3), 6.44 (1H, d, J = 2.1 Hz, H-8), 6.21 (1H, d, J = 2.0 Hz, H-6). ^{13}C-NMR (100 MHz, MeOH-d_4, TMS), δ_C: 182.5 (C-4), 165.0 (C-7), 164.6 (C-2), 161.8 (C-5), 158.0 (C-9), 149.6 (C-4′), 145.7 (C-3′), 122.3 (C-1′), 118.9 (C-6′), 115.4 (C-5′), 112.7 (C-2′), 103.9 (C-3), 102.5 (C-10), 98.7 (C-6), 93.6 (C-8). The data above were compared with those reported in the literature. So, compound **4** was identified as luteolin [23].

Compound **5**: yellow powder. LR-EIMS: *m/z*, 316.27 ($C_{16}H_{12}O_7$). ^{1}H-NMR (400 MHz, DMSO-d_6, TMS), δ_H: 12.47 (1H, s, HO-5), 10.77 (1H, s, HO-3), 9.74 (1H, s, HO-7), 9.43 (1H, s, HO-4′), 7.76 (1H, d, J = 2.2 Hz, H-2′), 7.69 (1H, dd, J = 2.2 Hz, 8.5 Hz, H-6′), 6.94 (1H, d, J = 8.5 Hz, H-5′), 6.48 (1H, d, J = 2.1 Hz, H-8), 6.20 (1H, d, J = 2.1 Hz, H-6), 3.85 (3H, s, CH_3-7′). ^{13}C-NMR (100 MHz, DMSO-d_6, TMS), δ_C: 164.4 (C-7), 161.2 (C-5), 156.6 (C-9), 149.3 (C-4), 147.8 (C-3′), 147.1 (C-2), 136.29 (C-3), 132.3 (C-4′), 122.4 (C-1′), 122.2 (C-6′), 116.0 (C-5′), 112.2 (C-2′), 103.5 (C-10), 98.8 (C-6), 94.1 (C-8), 56.2 (C-7′). The data above were compared with those reported in the literature. So, compound **5** was identified as isorhamnetin [24].

Compound **6**: off-White powder. LR-EIMS: *m/z*, 304.25 ($C_{15}H_{18}O_7$). ^{1}H-NMR (400 MHz, MeOH-d_4, TMS), δ_H: 6.98 (1H, d, J = 2.0 Hz, H-2′), 6.87 (1H, dd, J = 2.0 Hz, 8.2 Hz, H-6′), 6.82 (1H, d, J = 8.2 Hz, H-5′), 5.94 (1H, d, J = 2.1 Hz, H-8), 5.90 (1H, d, J = 2.1 Hz, H-6), 4.93 (1H, d, J = 11.5 Hz, H-2), 4.52 (1H, d, J = 11.5 Hz, H-3). ^{13}C-NMR (100 MHz, MeOH-d_4, TMS), δ_C: 197.0 (C-4), 167.3 (C-7), 163.9 (C-5), 163.1 (C-9), 154.7 (C-4′), 144.9 (C-5′), 128.5 (C-1′), 119.5 (C-2′), 114.7 (C-6′, 3′), 100.4 (C-10), 95.9 (C-6), 949 (C-8), 83.7 (C-2), 72.3 (C-3). The data

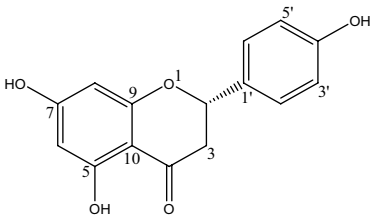

Naringenin
(*S*)-5,7-dihydroxy-2-(4-hydroxyphenyl)chroman-4-one

1

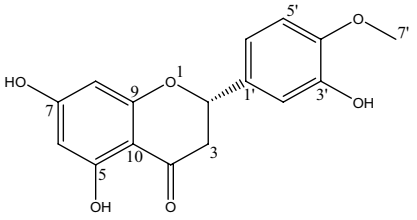

Hesperetin
(*S*)-5,7-dihydroxy-2-(3-hydroxy-4-methoxyphenyl)chroman-4-one

2

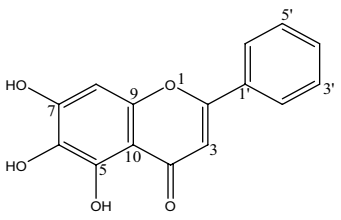

Baicalein
5,6,7-trihydroxy-2-phenyl-4*H*-chromen-4-one

3

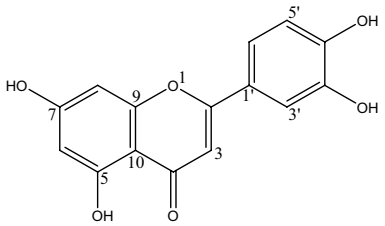

Luteolin
2-(3,4-dihydroxyphenyl)-5,7-dihydroxy-4*H*-chromen-4-one

4

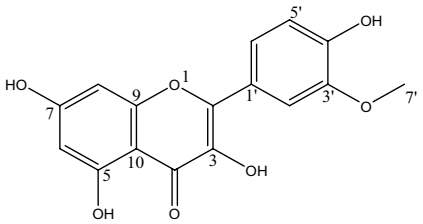

Isorhamnetin
3,5,7-trihydroxy-2-(4-hydroxy-3-methoxyphenyl)-4*H*-chromen-4-one

5

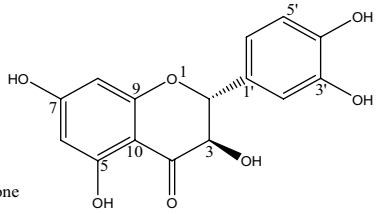

Taxifolin
(2*R*,3*R*)-2-(3,4-dihydroxyphenyl)-3,5,7-trihydroxychroman-4-one

6

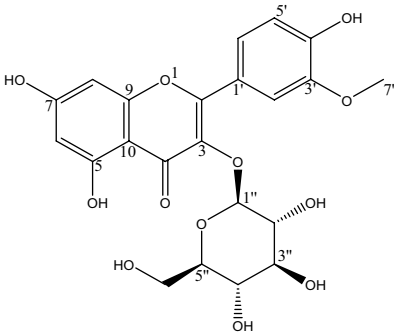

Isorhamnetin-3-O-β-D-Glucoside
5,7-dihydroxy-2-(4-hydroxy-3-methoxyphenyl)-3-(((2*S*,3*R*,4*S*,5*S*,6*R*)-3,4,5-trihydroxy-6-(hydroxymethyl)tetrahydro-2*H*-pyran-2-yl)oxy)-4*H*-chromen-4-one

7

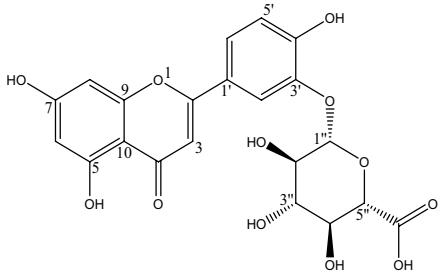

Luteolin-3'-D-glucuronide
(2*S*,3*S*,4*S*,5*R*,6*S*)-6-(5-(5,7-dihydroxy-4-oxo-4*H*-chromen-2-yl)-2-hydroxyphenoxy)-3,4,5-trihydroxytetrahydro-2*H*-pyran-2-carboxylic acid

8

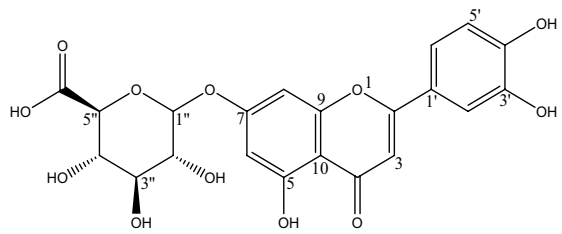

Luteolin-7-O-β-D-glucuronide
(2*S*,3*S*,4*S*,5*R*)-6-((2-(3,4-dihydroxyphenyl)-5-hydroxy-4-oxo-4*H*-chromen-7-yl)oxy)-3,4,5-trihydroxytetrahydro-2*H*-pyran-2-carboxylic acid

9

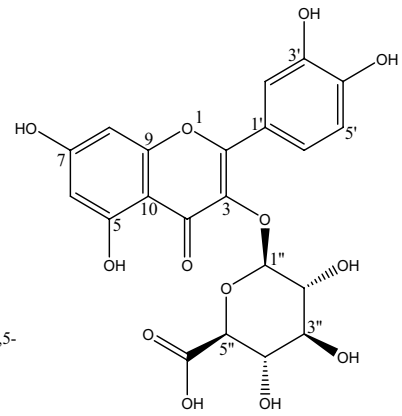

Quercetin-3-O-β-D-glucuronide
(2*S*,3*S*,4*S*,5*R*,6*S*)-6-((2-(3,4-dihydroxyphenyl)-5,7-dihydroxy-4-oxo-4*H*-chromen-3-yl)oxy)-3,4,5-trihydroxytetrahydro-2*H*-pyran-2-carboxylic acid

10

Fig. 1 Chemistry structures (2D) of compounds **1**–**10**

above were compared with those reported in the literature resulting in compound **6**, namely taxifolin [25].

Compound **7**: yellow powder. LR-EIMS: *m/z*, 478.41 ($C_{22}H_{22}O_{12}$). ^{1}H-NMR (400 MHz, MeOH-d_4, TMS), δ_H: 7.94 (1H, d, *J* = 2.1 Hz, H-2′), 7.60 (1H, dd, *J* = 2.1 Hz, 8.5 Hz, H-6′), 6.92 (1H, d, *J* = 8.5 Hz, H-5′), 6.40 (1H, d, *J* = 2.1 Hz, H-8), 6.21 (1H, d, *J* = 2.1 Hz, H-6), 5.44–5.39 (1H, m, H-1″), 3.96 (3H, s, CH_3-7′), 3.75 (1H, dd, *J* = 2.3 Hz, 12.0 Hz, H-6″α), 3.57 (1H, dd, *J* = 5.4 Hz, 12.0 Hz, H-6″β), 3.51–3.44 (2H, m, H-3″, 5″), 3.35–3.31 (5H, m, H-2″, OH-2″, 3″, 4″, 6″), 3.26 (1H, m, H-4″). ^{13}C-NMR (100 MHz, MeOH-d_4, TMS), δ_C: 178.0 (C-4), 165.0 (C-7), 161.7 (C-5), 157.2 (C-2), 157.1 (C-9), 149.5 (C-4′), 147.0 (C-3′), 133.9 (C-3), 122.4 (C-6′), 121.7 (C-1′), 114.6 (C-5′), 113.0 (C-2′), 104.3 (C-10), 102.3 (C-1″), 98.6 (C-6), 93.4 (C-8), 77.1 (C-5″), 76.7 (C-3″), 74.5 (C-2″), 70.1 (C-4″), 61.1 (C-6″), 55.4 (C-7′). The data above were compared with those reported in the literature. So, compound **7** was identified as isorhamnetin-3-*O*-β-D-glucoside [26].

Compound **8**: Light yellow powder. LR-EIMS: *m/z*, 462.363 ($C_{21}H_{18}O_{12}$). ^{1}H-NMR (400 MHz, DMSO-d_6, TMS), δ_H: 12.95 (1H, s, HO-6″), 10.84 (1H, s, HO-7), 9.73 (1H, s, HO-4′), 7.69 (1H, d, *J* = 2.2 Hz, H-2′), 7.65 (1H, d, *J* = 2.2 Hz, 8.4 Hz, H-6′), 7.00 (1H, d, *J* = 8.4 Hz, H-5′), 6.86 (1H, s, H-3), 6.51 (1H, d, *J* = 2.1 Hz, H-8), 6.21 (1H, d, *J* = 2.1 Hz, H-6), 5.26 (1H, d, *J* = 4.0 Hz, H-1″), 5.21 (1H, d, *J* = 7.2 Hz, H-5″), 4.07 (1H, d, *J* = 9.6 Hz, H-2″), 3.49–3.36 (5H, m, H-3″, 4″, OH-2″, 3″, 4″). ^{13}C-NMR (100 MHz, DMSO-d_6, TMS), δ_C: 181.6 (C-4), 170.2 (C-6″), 164.2 (C-7), 163.4 (C-2), 161.5 (C-5), 157.4 (C-9), 150.8 (C-4′), 145.2 (C-3′), 122.0 (C-1′), 121.6 (C-6′), 116.7 (C-5′), 113.9 (C-2′), 103.8 (C-10), 103.3 (C-3), 100.7 (C-1″), 98.9 (C-6), 94.1 (C-8), 75.5 (C-3″), 73.0 (C-2″), 71.4 (C-5″). The data above were compared with those reported in the literature resulting in compound **8**, namely luteolin-3′-D-glucuronide [27].

Compound **9**: yellow powder. LR-EIMS: *m/z*, 462.36 ($C_{21}H_{18}O_{12}$). ^{1}H-NMR (400 MHz, DMSO-d_6, TMS), δ_H: 13.01 (1H, s, HO-6″), 10.00 (1H, s, HO-3′), 9.45 (1H, s, HO-4′), 7.46 (1H, dd, *J* = 2.2 Hz, 8.4 Hz, H-6′), 7.43 (1H, d, *J* = 2.2 Hz, H-2′), 6.91 (1H, d, *J* = 8.4 Hz, H-5′), 6.82 (1H, d, *J* = 2.2 Hz, H-8), 6.76 (1H, s, H-3), 6.47 (1H, d, *J* = 2.2 Hz, H-6), 5.45 (1H, br.s, H-5″), 5.29 (1H, d, *J* = 7.0 Hz, H-1″), 4.05 (1H, d, *J* = 9.4 Hz, H-4″), 3.43–3.28 (5H, m, H-2″, 3″, OH-2″, 3″, 4″). ^{13}C-NMR (100 MHz, DMSO-d_6, TMS), δ_C: 181.9 (C-4), 170.1 (C-6″), 164.5 (C-2), 162.5 (C-7), 161.2 (C-5), 156.9 (C-9), 149.9 (C-4′), 145.8 (C-3′), 121.3 (C-1′), 119.1 (C-6′), 116.0 (C–5′), 113.5 (C-2′), 105.4 (C-10), 103.2 (C-3), 99.4 (C-1″), 99.1 (C-6), 94.5 (C-8), 75.6 (C-5″), 75.3 (C-3″), 72.7 (C-2″), 71.2 (C-4″). The data above were compared with those reported in the literature resulting in compound **9**, namely luteolin-7-*O*-β-D-glucuronide [28].

Compound **10**: yellow powder. LR-EIMS: *m/z*, 478.362 ($C_{21}H_{18}O_{13}$). ^{1}H-NMR (400 MHz, DMSO-d_6, TMS), δ_H: 12.57 (1H, s, HO-6″), 10.89 (1H, s, HO-7), 9.77 (1H, s, HO-3′), 9.23 (1H, s, HO-4′), 7.61 (1H, dd, *J* = 2.2 Hz, 8.5 Hz, H-6′), 7.53 (1H, d, *J* = 2.2 Hz, H-2′), 6.84 (1H, d, *J* = 8.5 Hz, H-5′), 6.41 (1H, d, *J* = 2.1 Hz, H-8), 6.21 (1H, d, *J* = 2.1 Hz, H-6), 5.50 (1H, d, *J* = 7.3 Hz, HO-5″), 5.29 (1H, br.s, H-1″), 3.57 (1H, d, *J* = 9.6 Hz, H-4″), 3.41–3.26 (5H, m, H-2″, 3″, OH-2″, 3″, 4″). ^{13}C-NMR (100 MHz, DMSO-d_6, TMS), δ_C: 177.2 (C-4), 168.8 (C-6″), 164.3 (C-7), 161.2 (C-5), 156.3 (C-2), 156.2 (C-9), 148.7 (C-4′), 145.0 (C-3′), 133.1 (C-3), 121.7 (C-6′), 120.9 (C-1′), 116.1 (C-2′), 115.2 (C-5′), 103.9 (C-10), 101.1 (C-1″), 98.8 (C-6), 93.6 (C-8), 76.0 (C-5″), 75.9 (C-3″), 73.8 (C-2″), 71.4 (C-4″). The data above were compared with those reported in the literature. So, compound **10** was identified as quercetin-3-*O*-β-D-glucuronide [29].

Average food intake, average stool excretion, stool morphology

During the experiment, the amount of food intake and stool excretion in the MOD group was significantly lower than that in the CON group. After treatment, the food intake and stool excretion of mice in the dosing group increased significantly and tended to be normal (Fig. S1a–b), and the effect was more obvious with the increase in dose. By observing the feces of mice in each group, it was found that the stool of the mice in the CON group were dry and long, brown in color, and the stool in the MOD group were fusiform, with a dark black-brown surface and an oily film feeling (Fig. S1c).

Facilitation of gastrointestinal transit in FD mice

By feeding a high-fat diet, mice will have gastrointestinal motility disorders. Through the data processing of gastric emptying rate and intestinal propulsion rate, and observing the gastrointestinal motility change index, it was found that compared with the CON group, the gastric emptying rate and intestinal propulsion rate of mice in the MOD group were reduced (Fig. S2). Compared with the MOD group, the two positive drug groups, the S.s L group, the S.s M group, and the S.s H group could accelerate gastric emptying and intestinal propulsion of mice ($P < 0.05$, $P < 0.01$, and $P < 0.001$), indicating that *S. salsa* decoction had a significant effect on food accumulation mice at normal doses, and the effect of high doses was stronger than that of low doses ($P < 0.001$).

Effects on the morphology of the colon in FD mice

The results showed that there were a large number of goblet cells in the colon tissue of the CON group, the goblet

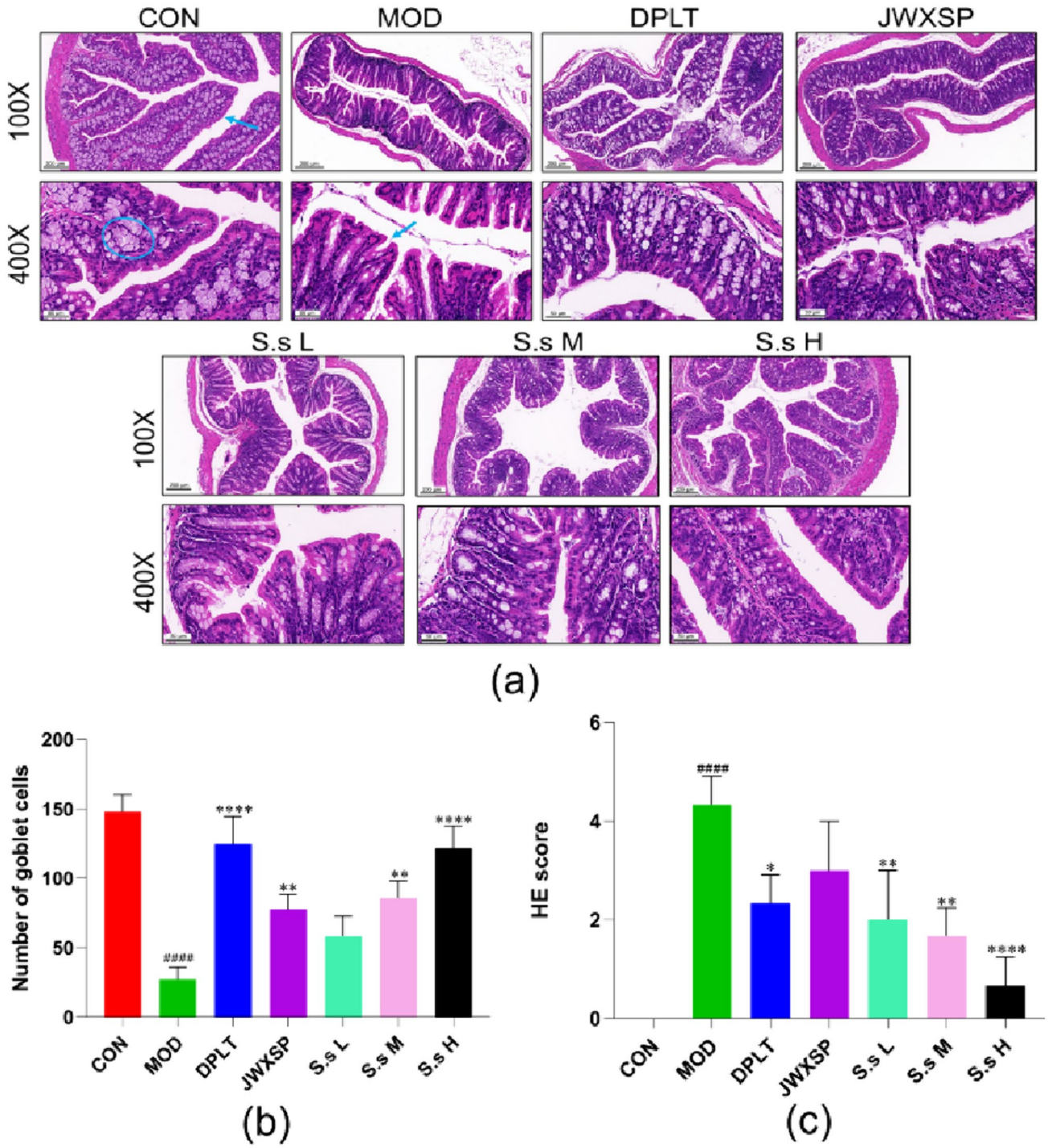

Fig. 2 Effects on the morphology of the colon in FD mice. **a** H&E staining in the stomach, 100 and × 400 magnification. **b** Number of goblet cells. **c** Statistical chart of HE score ($n = 3$). Data are expressed as mean ± SD ($n = 3$). #### $P < 0.0001$ compared to control group. * $P < 0.05$, ** $P < 0.01$ and **** $P < 0.0001$ compared to model group

cells were neat and numerous, and the intestinal mucosa and intestinal villi were arranged completely, tightly, and continuously (Fig. 2). Compared with the CON group, the number of goblet cells in the colon tissue of the MOD group was greatly reduced (Fig. 2b, $P < 0.0001$) the arrangement was loose, the intestinal mucosa was destroyed, the intestinal villi were loosely arranged, and necrosis fell off (Fig. 2c, $P < 0.0001$). After treatment, the histological structure of colon lesions in the two positive control groups was significantly improved (Fig. 2b, c ,

$P < 0.05$, $P < 0.001$ and $P < 0.0001$). The lesion location in the S.s L group, the S.s M group, and the S.s H group were also improved.

Effects on serum hormones in FD mice

Compared with the CON group, the hormone levels of 5-HT, CCK, NT, SS, VIP, and GT-17 in the MOD group were significantly increased (Fig. S3a–f), and the levels of CHE, MTL, and Ghrelin hormone were significantly decreased (Fig. S3g–i). After treatment with positive drugs, the average upward regulation of hormone content tended to be in the CON group, and the effect of the S.s H group was better than that of the S.s L group and even tended to be the positive drug group ($P < 0.001$ and $P < 0.0001$).

Effects on c-kit, SCF and GHRL proteins in colon tissues of FD mice

Western Blot method was used to detect c-kit, SCF, and GHRL proteins in the colonic tissues of mice in each group (Fig. 3a–d). Compared with the CON group, the expression of c-kit, SCF, and GHRL protein in colon tissue in the MOD group was reduced, which was statistically different ($P < 0.0001$). After treatment, the expression levels of the three proteins in the administration group were increased to varying degrees, and even the effect of the S.s L group was higher than that of the positive drug ($P < 0.0001$).

Gut microbiota

Community diversity analysis

The dilution curve and Alpha diversity index are commonly used to evaluate microbial diversity. Species richness and diversity were analyzed by dilution curve, Shannon index, and Simpson index (Fig. S4). When the dilution curve tended to be flat, it indicated that the sequencing data was reasonable and the amount of data was large enough (Fig. S4a). Both indexes showed that the community diversity of the MOD group was lower than the CON group. The community diversity was increased in the treatment groups. The effect of the JWXSP group was better than that of the DPLT group. In the *S. salsa* crude extract group, the effect gradually increased with the increase of dose, but the effect was worse than that of the positive drug (Fig. S4b and c).

Community composition analysis

Venn diagram showed the common OTU among groups, it showed that the species composition of *S. salsa* at high dose was significantly higher than that of the other two groups and the MOD group, indicating that *S. salsa* increased the species richness in the intestinal microbiota, and the effect was stronger with the increase of dose (Fig. 4a). The community Circos diagram reflected the distribution proportion of dominant species in different samples, and analyzed the dominant groups. Firmicutes and Bacteroidetes account for a relatively high proportion and were the dominant groups in each group of samples (Fig. 4b). The Bar graph of the

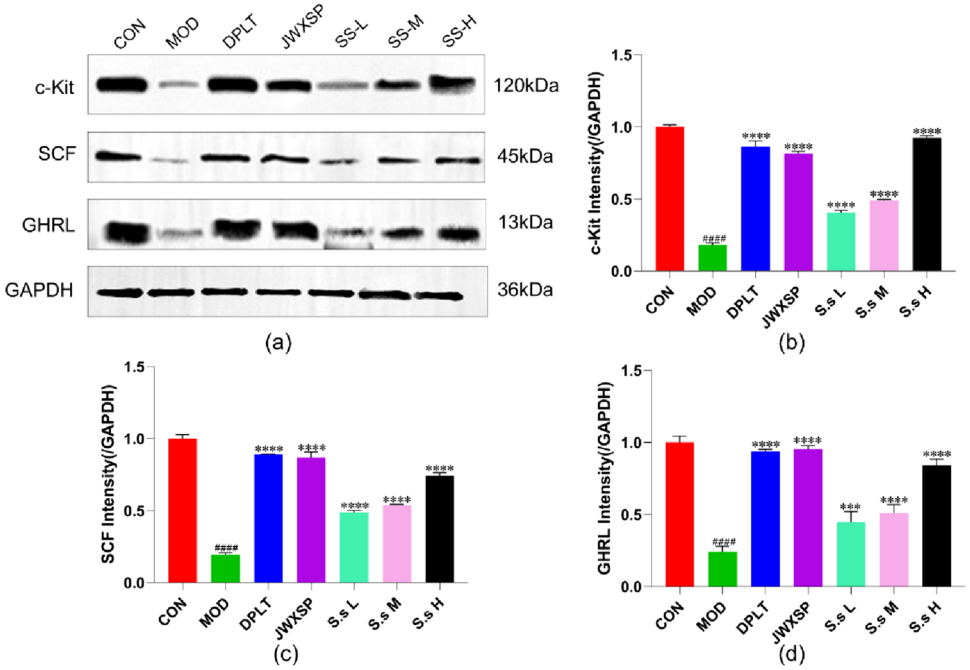

Fig. 3 Effects on c-kit, SCF and GHRL proteins in colon tissues of FD mice. **a** c-kit, SCF, GHRL and GAPDH western blot. **b** Grey value of c-Kit. **c** Grey value of SCF. **d** Grey value of GHRL. Data repeated 3 times. Data are expressed as mean ± SD ($n = 3$). #### $P < 0.0001$ compared to control group. *** $P < 0.001$ and **** $P < 0.0001$ compared to model group

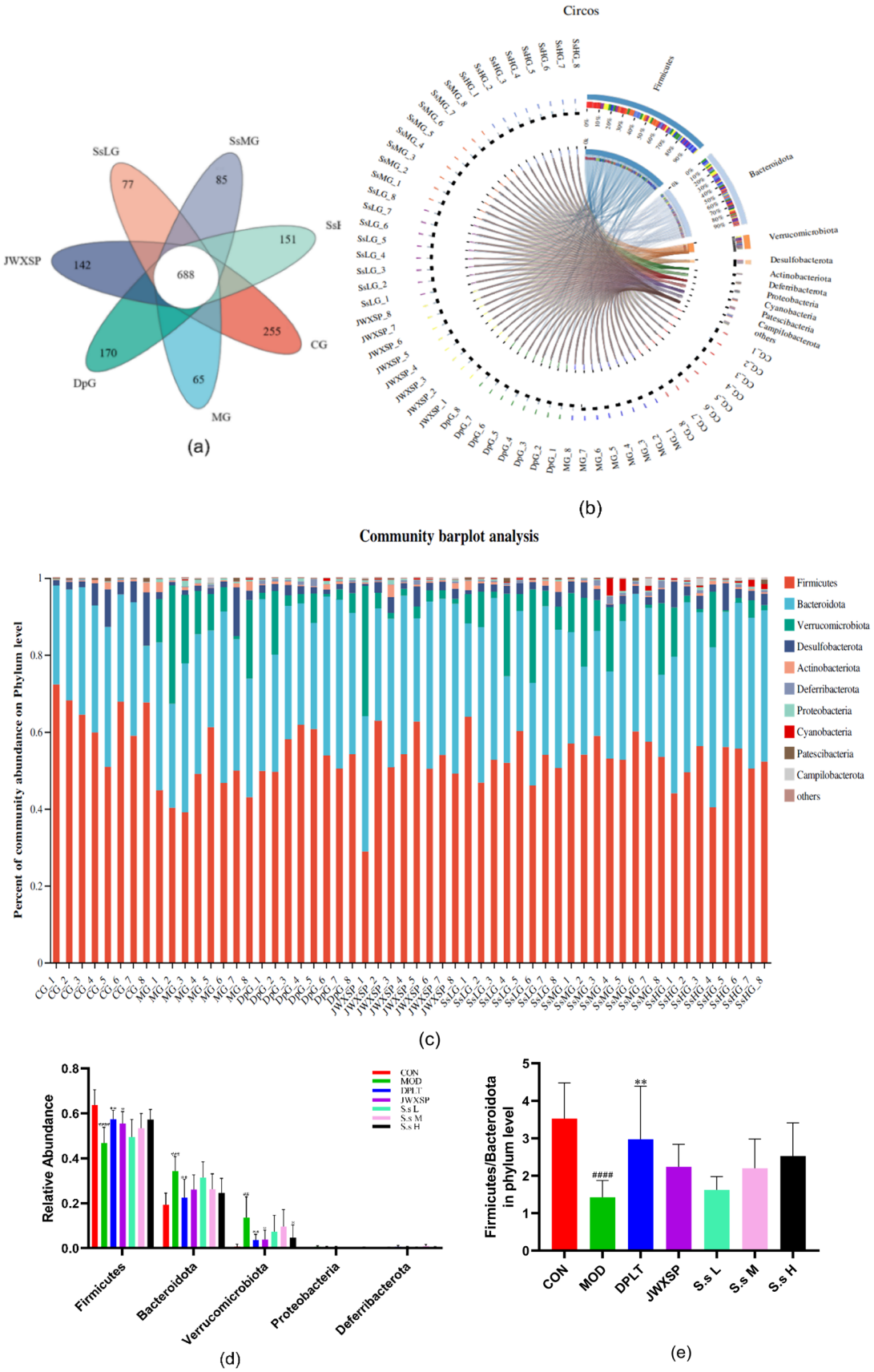
SsLG
SsMG
SsHG
JWXSP
CG
DpG
MG
77
85
151
142
688
255
170
65
(a)
Circos
Firmicutes
Bacteroidota
Verrucomicrobiota
Desulfobacterota
Actinobacteriota
Deferribacterota
Proteobacteria
Cyanobacteria
Patescibacteria
Campilobacterota
others
(b)
Community barplot analysis
Percent of community abundance on Phylum level
Firmicutes
Bacteroidota
Verrucomicrobiota
Desulfobacterota
Actinobacteriota
Deferribacterota
Proteobacteria
Cyanobacteria
Patescibacteria
Campilobacterota
others
(c)
Relative Abundance
CON
MOD
DPLT
JWXSP
S.s L
S.s M
S.s H
Firmicutes
Bacteroidota
Verrucomicrobiota
Proteobacteria
Deferribacterota
(d)
Firmicutes/Bacteroidota in phylum level
####
**
CON
MOD
DPLT
JWXSP
S.s L
S.s M
S.s H
(e)

◂**Fig. 4** Analysis of gut microbiota community composition of *S. salsa* on FD mice. **a** Venn diagram. **b** Circos diagram. **c** Percent of Community barplot analysis on Phylum level. **d** Relative abundance on Phylum level. **e** Firmicutes/Bacteroidetes in Phylum level. Data repeated 3 times. Data are expressed as mean ± SD ($n = 3$). ### $P < 0.001$ and #### $P < 0.0001$ compared to control group. * $P < 0.05$ and ** $P < 0.01$ compared to model group

community showed visually what microorganisms were contained in each sample at the phylum level and the relative abundance of each microorganism in the sample. At the phylum level, Firmicutes, Bacteroidota, and Verrucomicrobiota are the dominant microbiota, accounting for a large proportion (Fig. 4c, d). Compared with the CON group, the abundance of Firmicutes in the MOD group was lower, and the abundance of Bacteroidetes was higher (Fig. 4d). *S. salsa* solution significantly inhibited the decrease of Firmicutes and the increase of Bacteroidetes. In contrast, the inhibitory effect of the DPLT group was not obvious. In the MOD group, the relative abundance of Verrucomicrobiota was significantly higher than that in the CON group. After treatment, the abundance of Verrucomicrobiota was significantly reduced (Fig. 4d). By observing the ratio of Firmicutes/Bacteroidetes (F/B), it was found that the MOD group showed a downward trend, which could be reversed in the administration group, and the S.s L group was close to the positive drug group (Fig. 4e).

Sample comparison difference analysis

β-Diversity is mainly used to evaluate the structure and composition of different intestinal microbiota. In principal component analysis (PCA), the more similar the species composition of the sample, the closer the distance reflected in the PCA diagram. Compared with the CON group, the species composition of the two groups was significantly different, and the composition was not similar. After treatment, the species composition of the samples in the administration group was not significantly different from that in the CON group, and the similarity of the composition was increased. Among them, the species composition of the S.s L group and the CON group were the most similar. (Fig. S5).

LEfSe analysis

LEfSe analysis was used to determine the specificity of intestinal microbiota in each group (LDA > 4). In the CON group, three categories were significantly affected ($P < 0.0001$). Under the intervention of the S.s M group, four categories were significantly affected ($P < 0.001$ and $P < 0.0001$), among which Firmicutes was a differential microbial group, while five dominant categories in the MOD group were affected (Fig. S6, $P < 0.001$ and $P < 0.0001$). These results suggested that *S. salsa* can regulate the structure of intestinal microbiota and played a role in the host.

Discussion

FD is considered to be one of the most common diseases in clinic, with a high incidence in the general population. In recent years, with the improvement of people's living standards and the great variety of food, people often intake high-fat, high protein and other foods, which lead to diet disorders and can cause or exacerbate diet stagnation type functional dyspepsia [30]. Clinically, the commonly used methods for the treatment of FD are acid suppressants, antidepressants, neuromodulators, and prokinetic drugs [30]. At present, natural herbal medicine has also been proven to be effective in the treatment of FD, and the therapeutic effect is equivalent. Even Chinese herbal medicine is more effective than prokinetic drugs in reducing overall symptoms [31]. Studies have shown that peppermint oil and *Fructus aurantii* can effectively improve gastrointestinal peristalsis and regulate neurohormone abnormalities [7, 32]. Therefore, we speculate that natural traditional drugs, with the advantages of more safety, will become a common means of treating FD.

S. salsa has a long history for applying and is rich in chemical composition and medicinal value. As early as the Ming Dynasty in China, it was recorded that "*S. salsa* was described with salty in flavor and cold in nature, clear away heat and dissipates the food accumulation". However, in modern research, using the keywords "*Suaeda salsa*", "Pharmacology", "functional dyspepsia" and "gastrointestinal function" to search scientific databases such as "Web of science", "PubMed", "Springer", "ScienceDirect", "Bing international", and "ACS", it was found that the digestion and accumulation effect of *S. salsa*, even for improving gastrointestinal function, had not been reported yet. Therefore, we established a mice model of FD by feeding a high-fat and high-protein diet to explore the mechanism of digesting food and dissipating the food accumulation of *S. salsa*. During the modeling period, the mice suffered from decreased food intake and stool excretion, changes in physical signs, gastrointestinal dysfunction, and other symptoms. After treatment, the food intake, stool excretion and stool morphology of mice returned to normal, and the gastric emptying rate and intestinal propulsion rate were significantly improved, which successfully improved the gastrointestinal motility disorder of mice. With the increase of the dosage, the effect is better.

Brain-gut peptide, as an important factor in the brain-gut axis, plays an important regulatory role in all aspects of brain-gut axis [33]. Brain-gut peptides of the gastrointestinal system and central nervous system regulate gastrointestinal motility, sensation, secretion, absorption, and other complex functions through endocrine, neurosecretory, and paracrine

functions [34]. 5-HT is synthesized in central neurons and intestinal chromaffin cells of animals (including the human) digestive tract, and is widely distributed in the gastrointestinal tract, central nervous system, and platelets. 90% of 5-HT in the gastrointestinal tract is used to stimulate the intestinal muscle plexus and affect the rate of intestinal peristalsis. The rest is synthesized in the serotonergic neurons of the central nervous system, which can regulate appetite and mood [35]. 5-HT receptors are complex, and different receptors have different pharmacological activities. When acting on smooth muscle, the 5-HT2 receptor of gastrointestinal smooth muscle and the 5-HT4 receptor of ganglion cells in intestinal wall can cause contraction of gastrointestinal smooth muscle, increase gastrointestinal tension and accelerate intestinal peristalsis [36]. When acting on the nervous system, the increase of 5-HT content can cause a series of behaviors such as drowsiness and sedation [37]. Previous studies have shown that the increase of 5-HT level can cause satiety, which is helpful in reducing food intake and intestinal peristalsis [38]. Cholecystokinin (CCK) is a peptide hormone related to the gastrointestinal (GI) system, which is released by intestinal endocrine cells I [39]. CCK can regulate the release of bile acids, inhibit gastric emptying, inhibit postprandial gastric acid secretion, and slow down gastrointestinal peristalsis [40]. Studies have confirmed that feeding a high-fat diet for 8 weeks can reduce ghrelin and increase CCK in rats' plasma, which can improve gastrointestinal motility and promote digestion in FD rats by reducing the concentration of CCK in gastrointestinal tissue [41, 42]. Neurotensin (NT) is a small peptide with pleiotropic function, which is mainly produced in hypothalamic, pituitary and ileal neuroendocrine cells [43]. It is an important regulator of brain-gut peptide. NT can reduce food intake and induce anorexia by regulating the two receptors NTSR1 and NTSR3 in the intestine. At the same time, NT can also increase the time course of anorexia by activating some brain regions and central nervous system that control appetite. Therefore, NT signaling has gut brain axis significance [44]. Studies have confirmed that the content of NT in the serum of mice fed with a high-fat diet is significantly increased. NT can promote the absorption of intestinal fat in the gastrointestinal tract by regulating the release of neurotransmitters in the central nervous system [45]. Somatostatin (SS) is a typical brain-gut peptide. It is not only released by the hypothalamus and inhibits the release of pituitary growth hormone, but also released by D cells in gastrointestinal mucosa [46]. The gastrointestinal tract is the largest secretory organ, and most SS endocrine cells are distributed. They regulate gastrointestinal function and inhibit intestinal peristalsis by releasing gastrointestinal hormones [47]. Vasoactive intestinal peptide (VIP) is an intestinal peptide hormone, which is widely distributed in the central nervous system and intestinal nervous system and is mainly released by intestinal neurons [48]. VPAC1 and VPAC2, two receptors of VIP, are closely related to gastrointestinal motility. The activation of VPAC2 in gastrointestinal smooth muscle can increase gastrointestinal motility. VIP can also inhibit gastric acid secretion, contract gastrointestinal smooth muscle and reduce gastrointestinal transport function by activating VPAC1 [49]. GT-17 is a gastrin subgroup consisting of 17 amino acids, which is produced only by antral G cells [50]. More than 95% of the bioactive gastrin secreted by G cells in the gastric antrum is amidated gastrin. Among them, 85% is GT-17 [51]. GT-17 plays an important role in regulating gastrointestinal function and maintaining its structural integrity. It is the main stimulant of gastric acid secretion [52]. Studies have shown that the content of GT-17 in patients with functional dyspepsia caused by short-term discontinuation of proton pump inhibitor (PPI) increased significantly [53]. Cholinesterase (CHE) mainly exists in the synaptic space of cholinergic nerve endings. As a direct nutritional factor, it regulates intestinal health [54]. Motilin (MTL) is produced in the endocrine cells of the upper intestinal mucosa. It is a gastrointestinal hormone secreted by the duodenum and is an important regulator of gastrointestinal (GI) motility [55]. The potential mechanism of MTL on the gastrointestinal tract is mainly to stimulate neural pathways, intestinal serotonergic neurons and intestinal chromaffin cells, release adrenergic receptors, and serotonin (5-HT) receptors, and stimulate the muscular plexus of the living intestine through vagal nerve outgoing neurons to cause the contraction of the stomach and upper intestine [56]. It has been reported that the intestinal motility disorder caused by constipation can be effectively alleviated through the increase of MTL hormone content [57]. Ghrelin is a brain-gut hormone with a wide range of physiological functions. Ghrelin-producing cells are distributed throughout the gastrointestinal tract [58]. Our experimental results showed that the serum levels of 5-HT, CCK, NT, SS, VIP, and GT-17 in the MOD group were significantly higher than those in the CON group, while the level of CHE, MTL, and ghrelin was significantly lower. After administration of *S. salsa*, the contents of various hormones were significantly changed and gradually tended to normal levels. It can be seen that *S. salsa* has a significant regulatory effect on improving gastrointestinal motility. At the same time, it was found that the effect became more significant with the increase of the dose of the liquid.

C-kit and SCF proteins are key proteins regulating gastrointestinal function. SCF is a dimer molecule that binds to receptor c-kit and activates its biological function [59]. It has been reported that the interaction of the two can promote gastrointestinal motility, accelerate gastric emptying, reduce visceral hypersensitivity, and improve duodenal microinflammation, so as to achieve the purpose of treating FD [60]. GHRL protein is a powerful appetite stimulant, which is widely distributed in the gastrointestinal tract. It

can stimulate appetite and promote intestinal peristalsis, and help regulate energy homeostasis [61]. The results showed that the expressions of c-kit, SCF, and GHRL in colon tissue were significantly increased compared with the MOD group.

Interstitial cells of Cajal (ICCs) are a very special kind of interstitial cells between the enteric nervous system (ENS) and smooth muscle cells. They are slow-wave pacemaker cells in the gastrointestinal tract and play an important role in regulating the transmission of intestinal nerve signals to effector smooth muscle cells. It is currently considered to be the target of drug intervention for FD patients [62, 63]. C-kit mainly exists in ICCs and is a specific marker of ICCs in the gastrointestinal tract. SCF is a ligand factor of c-kit and regulates the proliferation of ICCs. Studies have shown that when the expressions of c-kit and SCF proteins increase, they can promote the proliferation of ICCs and improve gastrointestinal motility [64]. SS is produced by hypothalamic and pancreatic cells. In the gastrointestinal tract, SS can inhibit the secretion of CCK, Gastin, and VIP, as well as the release of gastric acid [46], thereby regulating gastrointestinal peristalsis. CCK, VIP, GT-17, MTL and ghrelin are widely distributed in the gastrointestinal nervous system and regulate gastrointestinal motility. As a neurotransmitter released by the gastrointestinal nerve, MTL can combine with the receptors on ICCs, promote the depolarization of smooth muscle cells, and accelerate gastrointestinal transport [65]. C-kit and SCF regulate gastrointestinal hormones, accelerate intestinal peristalsis, and improve FD through the smooth muscle signal pathway of intestinal neuronal system ICCs [65]. 5-HT can induce the proliferation of ICCs and promote gastrointestinal peristalsis through the 5-HT_{2B} receptor [66]. At the same time, 5-HT, as a central neurotransmitter, decreased expression of 5-HT will lead to depression, reduce appetite, and slow intestinal peristalsis. Studies have confirmed that it can improve anorexia by antagonizing 5-HT, so as to restore the secretion of GHRL protein [67]. ICCs exert pacemaker activity mediated by intracellular Ca^{2+} oscillation and promote gastrointestinal motility. The function of ICCs is related to the current of voltage-dependent ion channels, mainly mediated by c-kit and SCF [68]. Studies have confirmed that CCK and NT can also regulate pacemaker current by releasing and activating Ca^{2+}. CCK mainly induces calcium signal transduction in ICCs and enhances gastrointestinal peristalsis through the release of Ca^{2+} stored in inositol 1,4,5-triphosphate ($InsP_3R$) and protein kinase C (PKC) [69]. NT regulates pacemaker currents through the activation of non-selective cation channels by intracellular Ca^{2+} release from neurotensin receptor 1 [69]. GHRL protein produces ghrelin and obestatin. Ghrelin is mainly produced in the endocrine cells of gastric mucosa, and then secreted into plasma. Ghrelin binds to its receptor GHSR and promotes gastric peristalsis and eating [70].

Compared with a low-fat diet, a high-fat diet can reduce the diversity of intestinal microbiota in humans and rodents [71]. 16S rDNA sequence analysis showed that at the phylum level, Firmicutes and Bacteroides were the dominant microbiota in the intestine. Compared with the CON group, the abundance of beneficial Firmicutes in the MOD group decreased, while the abundance of Bacteroidetes and Verrucomicrobiota increased. *S. salsa* inhibited the decrease of Firmicutes abundance, increased the abundance of Bacteroidetes and Verrucomicrobiota, improved the imbalance of intestinal microbiota, and restored the imbalance structure of intestinal microbiota [8]. The proportion of Firmicutes and Bacteroidetes is a general indicator of health, which is confirmed to be closely related to FD [72, 73]. By observing the ratio of Firmicutes/Bacteroidetes (F/B), it was found that the MOD group showed a downward trend, which could be significantly reversed in the medication group. The above intestinal microbiota are producers of short-chain fatty acids (SCFA), which are involved in the regulation of microbiota balance and gastrointestinal function [74]. Among them, Firmicutes is the main source of butyrate [75]. Butyrate performs its important functions in the gastrointestinal tract, especially maintaining the integrity of the intestinal wall and improving gastrointestinal motility [76]. Studies have confirmed that butyrate has a better effect in restoring intestinal motility [77]. Propionic acid is the main component of short-chain fatty acids produced by Bacteroidetes [78], which can reduce intestinal peristalsis [79]. Therefore, regulating the structure of intestinal microbiota can effectively improve gastrointestinal function, and then improve FD.

The physiological activities of the gastrointestinal tract are regulated by the enteric nervous system, central nervous system, and autonomic nervous system in a variety of ways. It has been reported that the brain-gut-gut microbiota axis is formed by the interaction of the brain-nervous system, gut, and gut microbiota [80]. The structural changes of the intestinal microbiota will cause changes in the physiological activities of the gastrointestinal tract, and then transmit the stimulation to the central nervous system, which can regulate various physiological and pathological activities in the intestinal tract. Changes in central nervous system activity can also regulate gastrointestinal peristalsis, immunity, hormone secretion, and other functions, and affect the composition of the gastrointestinal microbiota. Studies have confirmed that SCFAs are metabolites of gastrointestinal microbiota and are generally considered to be the key medium for communication between the central nervous system and the gut [81]. SCFAs induces intestinal secretion of G protein-coupled receptors, which are transmitted to the central nervous system through the vagus nerve pathway to play anti-inflammatory or other immune effects [82].

Conclusion

In this paper, the phytochemical and biological activities of *S. salsa* were studied. Ten flavonoids were identified from the ethyl acetate layer and water-saturated *n*-butanol layer of the stems and branches of *S. salsa*. In order to explore the effect of *S. salsa* on digesting food and dissipating food accumulation, after a short-term high-fat diet feeding mice, the gastrointestinal function movement was abnormal. The crude extract of *S. salsa* can reduce gastrointestinal dysfunction and improve food accumulation by regulating "brain-gut-gut microbiota". It provides a basis for the subsequent application of medicinal plants or the development of functional food. It is worth noting that this report first explored the therapeutic effect of *S. salsa* on FD and explained the related mechanism.

Supplementary Information The online version contains supplementary material available at https://doi.org/10.1007/s00394-024-03401-2.

Acknowledgements The research was financially supported by the Science and Technology Department of Jilin Province (file no.: 20230402047GH) for providing research grant to carry out related research work.

Author contributions Zhang Wenjun: Writing-original draft, conceptualization. Wang Xueyu: Writing-original draft, conceptualization. Yin Shuanghui: Investigation, methodology. Wang Ye: Software. Li Yong: Writing—review & editing. Ding Yuling: Writing—review & editing, conceptualization, supervision. Zhang Wenjun and Wang Xueyu: Contributed equally to this work.

Data availability The authors declare that the data supporting the findings of this study are available within the paper and its Supplementary Information files. Should any raw data files be needed in another format they are available from the corresponding author upon reasonable request.

Declarations

Conflict of interest The authors declare no conflict of interest pertaining to this research paper.

Ethics approval All animal experiments were carried out by the relevant animal practice norms and regulations of Changchun University of Chinese Medicine, China, and had passed the approval of animal experiment ethics review of Changchun University of Chinese Medicine (approval number: 2022527), and the license number for experimental animals is SYXK (Ji) 2018–0014.

References

1. He Q, Liu C, Wang T, Sun J, Zhou X, Wang Y, Ma L, Wan J (2020) Research on mechanism of the effect of charred hawthorn on digestive by SCF_c-kit pathway. https://doi.org/10.21203/rs.3.rs-138593/v1
2. Xian F, Liu T, Bai C, Yang G, Ma X, Wang B, Huang L, Liu S, Zhen J, He J, Yu H, Ma Y, Wang T, Gu X (2021) Effect of Yinlai Decoction on the metabolic pathways in the lung of high-calorie diet-induced pneumonia rats. J Tradit Chin Med Sci 8(1):4–16. https://doi.org/10.1016/j.jtcms.2021.01.008
3. Medić B (2021) Modern approach to dyspepsia. Acta Clin Croat 60(4):731–738. https://doi.org/10.20471/acc.2021.60.04.21
4. Tziatzios G, Gkolfakis P, Papanikolaou IS, Mathur R, Pimentel M, Giamarellos-Bourboulis EJ, Triantafyllou K (2020) Gut microbiota dysbiosis in functional dyspepsia. Microorganisms 8(5):691. https://doi.org/10.3390/microorganisms8050691
5. Malagelada Juan R (2020) The brain-gut team. Dig Dis 38(4):293–298. https://doi.org/10.1159/000505810
6. Liu Y-W, Hui H-Y, Tan Z-J (2019) Gastrointestinal peptide hormones associated with brain-intestinal axis. World Chinese Journal of Digestology 27(16):1007–1012. https://doi.org/10.11569/wcjd.v27.i16.1007
7. Zhu J, Tong H, Ye X, Zhang J, Huang Y, Yang M, Zhong L, Gong Q (2020) The effects of low-dose and high-dose decoctions of *Fructus aurantii* in a rat model of functional dyspepsia. Med Sci Monit 26:e919815. https://doi.org/10.12659/msm.919815
8. Zhang X, Liu W, Zhang S, Wang J, Yang X, Wang R, Yan T, Wu B, Du Y, Jia Y (2022) Wei-Tong-Xin ameliorates functional dyspepsia via inactivating TLR4/MyD88 by regulating gut microbial structure and metabolites. Phytomedicine 102:154180. https://doi.org/10.1016/j.phymed.2022.154180
9. Osadchiy V, Martin CR, Mayer EA (2019) Gut microbiome and modulation of CNS function. Compr Physiol 10(1):57–72. https://doi.org/10.1002/cphy.c180031
10. Rhee SH, Pothoulakis C, Mayer EA (2009) Principles and clinical implications of the brain–gut–enteric microbiota axis. Nat Rev Gastroenterol Hepatol 6(5):306–314. https://doi.org/10.1038/nrgastro.2009.35
11. Xuemin Z (2017) Ben Cao Gang Mu Shi Yi, vol 3. China Classics Publishing House, Beijing
12. Wang X, Shao X, Zhang W, Sun T, Ding Y, Lin Z, Li Y (2022) Genus *Suaeda*: advances in phytology, chemistry, pharmacology and clinical application (1895–2021). Pharmacol Res 179:106203. https://doi.org/10.1016/j.phrs.2022.106203
13. Lan H, Wang H, Chen C, Hu W, Ai C, Chen L, Teng H (2023) Flavonoids and gastrointestinal health: single molecule for multiple roles. Crit Rev Food Sci Nutr. https://doi.org/10.1080/10408398.2023.2230501
14. Wu L, Jin X, Zheng C, Ma F, Zhang X, Gao P, Gao J, Zhang L (2023) Bidirectional effects of Mao Jian green tea and its flavonoid glycosides on gastrointestinal motility. Foods 12(4):854. https://doi.org/10.3390/foods12040854
15. Wang Y, JIA Q, Guo L, GU C, Li L, Wang X, Ling J (2022) Network pharmacological analysis of the mechanism of action of fructus aurantii immaturus in the treatment of functional dyspepsia. Tradit Chin Drug Res Clin Pharmacol 33(5):666–673. https://doi.org/10.19378/j.issn.1003-9783.2022.05.013
16. Bian Y, Lei J, Zhong J, Wang B, Wan Y, Li J, Liao C, He Y, Liu Z, Ito K, Zhang B (2022) Kaempferol reduces obesity, prevents intestinal inflammation, and modulates gut microbiota in high-fat diet mice. J Nutr Biochem 99:108840. https://doi.org/10.1016/j.jnutbio.2021.108840
17. Horai Y, Kakimoto T, Takemoto K, Tanaka M (2017) Quantitative analysis of histopathological findings using image processing software. J Toxicol Pathol 30(4):351–358. https://doi.org/10.1293/tox.2017-0031
18. Liu YJ, Tang B, Wang FC, Tang L, Lei YY, Luo Y, Huang SJ, Yang M, Wu LY, Wang W, Liu S, Yang SM, Zhao XY (2020) Parthenolide ameliorates colon inflammation through regulating Treg/Th17 balance in a gut microbiota-dependent manner. Theranostics 10(12):5225–5241. https://doi.org/10.7150/thno.43716
19. Zhuang H, Lv Q, Zhong C, Cui Y, He L, Zhang C, Yu J (2021) Tiliroside ameliorates ulcerative colitis by restoring the M1/M2

macrophage balance via the HIF-1α/glycolysis pathway. Front Immunol 12:649463. https://doi.org/10.3389/fimmu.2021.649463
20. Wang M, Wang YN, Wang HQ, Yang WQ, Ma SG, Li Y, Qu J, Liu YB, Yu SS (2023) Chemical constituents from leaves of *Craibiodendron yunnanense*. China J Chin Materia Med 48(4):978–984. https://doi.org/10.19540/j.cnki.cjcmm.20220608.201
21. Asai T, Matsukawa T, Ishihara A, Kajiyama S (2016) Isolation and characterization of wound-induced compounds from the leaves of *Citrus hassaku*. J Biosci Bioeng 122:208–212. https://doi.org/10.1016/j.jbiosc.2016.01.006
22. Chethankumara GP, Nagaraj K, Krishna V, Krishnaswamy G (2021) Isolation, characterization and in vitro cytotoxicity studies of bioactive compounds from *Alseodaphne semecarpifolia* Nees. Heliyon 7(6):e07325. https://doi.org/10.1016/j.heliyon.2021.e07325
23. Yang L, Wang C, Chen J, Qiu J, Du C, Wei Y, Hao X, Gu W (2023) Chemical constituents and bioactivitie of whole plant of *Primulina eburnea* from Guizhou. Chinese Traditional and Herbal Drugs 54:3430–3437. https://doi.org/10.7501/j.issn.0253-2670.2023.11.005
24. Delgado-Núñez EJ, Zamilpa A, González-Cortazar M, Olmedo-Juárez A, Cardoso-Taketa A, Sánchez-Mendoza E, Tapia-Maruri D, Salinas-Sánchez DO, Mendoza-de Gives P (2020) Isorhamnetin: a nematocidal flavonoid from *Prosopis laevigata* leaves against *Haemonchus contortus* eggs and larvae. Biomolecules 10(5):773. https://doi.org/10.3390/biom10050773
25. Peng Z-C, He J, Pan X-G, Ye X-S, Li X-X, Yin W-F, Zhang W-K, Xu J-K (2021) Isolation and identification of chemical constituents from fruit of *Cornus officinalis*. Chinese Traditional and Herbal Drugs. https://doi.org/10.7501/j.issn.0253-2670.2021.15.005
26. Zaher AM, Sultan R, Ramadan T, Amro A (2020) New antimicrobial and cytotoxic benzofuran glucoside from *Senecio glaucus* L. Nat Prod Res 36(1):136–141. https://doi.org/10.1080/14786419.2020.1768089
27. Heitz A, Carnat A, Fraisse D, Carnat A-P, Lamaison J-L (2000) Luteolin 3′-glucuronide, the major flavonoid from Melissa officinalis subsp. officinalis. Fitoterapia 71(2):201–202. doi:https://doi.org/10.1016/s0367-326x(99)00118-5
28. Xu Z, HE Ming-zhen, Yao M, Wang Z, Ouyang H, Li Z, Yang S, Li J, Feng Y (2023) Study on chemical constituents of *Ainsliaea fragrans*. Chinese Traditional and Herbal Drugs 54:1728–1735. https://doi.org/10.7501/j.issn.0253-2670.2023.06.004
29. Zhang XF, Thuong PT, Jin W, Su ND, Sok DE, Bae K, Kang SS (2005) Antioxidant activity of anthraquinones and flavonoids from flower of *Reynoutria sachalinensis*. Arch Pharmacal Res 28(1):22–27. https://doi.org/10.1007/Bf02975130
30. Amerikanou C, Kleftaki S-A, Valsamidou E, Chroni E, Biagki T, Sigala D, Koutoulogenis K, Anapliotis P, Gioxari A, Kaliora AC (2023) Food, dietary patterns, or is eating behavior to blame? Analyzing the nutritional aspects of functional dyspepsia. Nutrients 15(6):1544. https://doi.org/10.3390/nu15061544
31. Ho L, Zhong CCW, Wong CHL, Wu JCY, Chan KKH, Wu IXY, Leung TH, Chung VCH (2021) Chinese herbal medicine for functional dyspepsia: a network meta-analysis of prokinetic-controlled randomised trials. Chinese Medicine 16(1):140. https://doi.org/10.1186/s13020-021-00556-6
32. Kim YS, Kim J-W, Ha N-Y, Kim J, Ryu HS (2020) Herbal therapies in functional gastrointestinal disorders: a narrative review and clinical implication. Front Psych 11:601. https://doi.org/10.3389/fpsyt.2020.00601
33. Holzer P, Reichmann F, Farzi A (2012) Neuropeptide Y, peptide YY and pancreatic polypeptide in the gut–brain axis. Neuropeptides 46(6):261–274. https://doi.org/10.1016/j.npep.2012.08.005
34. Zeng WW, Yang F, Shen WL, Zhan C, Zheng P, Hu J (2022) Interactions between central nervous system and peripheral metabolic organs. Sci China Life Sci 65(10):1929–1958. https://doi.org/10.1007/s11427-021-2103-5
35. Juza R, Vlcek P, Mezeiova E, Musilek K, Soukup O, Korabecny J (2020) Recent advances with 5-HT3 modulators for neuropsychiatric and gastrointestinal disorders. Med Res Rev 40(5):1593–1678. https://doi.org/10.1002/med.21666
36. Spencer NJ, Keating DJ (2022) Role of 5-HT in the enteric nervous system and enteroendocrine cells. Br J Pharmacol. https://doi.org/10.1111/bph.15930
37. De Deurwaerdere P, Di Giovanni G (2021) 5-HT interaction with other neurotransmitters: an overview. Prog Brain Res 259:1–5. https://doi.org/10.1016/bs.pbr.2021.01.001
38. Liu N, Sun S, Wang P, Sun Y, Hu Q, Wang X (2021) The mechanism of secretion and metabolism of gut-derived 5-hydroxytryptamine. Int J Mol Sci 22(15):7931. https://doi.org/10.3390/ijms22157931
39. Okonkwo O, Zezoff D, Adeyinka A (2023) Biochemistry, cholecystokinin. In: StatPearls [Internet]. StatPearls Publishing, Treasure Island, FL
40. Cawthon CR, de La Serre CB (2021) The critical role of CCK in the regulation of food intake and diet-induced obesity. Peptides 138:170492. https://doi.org/10.1016/j.peptides.2020.170492
41. Özdemir-Kumral ZN, Koyuncuoğlu T, Arabacı-Tamer S, Çilingir-Kaya ÖT, Köroğlu AK, Yüksel M, Yeğen BÇ (2021) High-fat diet enhances gastric contractility, but abolishes nesfatin-1-induced inhibition of gastric emptying. J Neurogastroenterol Motil 27(2):265–278. https://doi.org/10.5056/jnm20206
42. Liang QK, Mao LF, Du XJ, Li YX, Yan Y, Liang JJ, Liu JH, Wang LD, Li HF (2018) Pingwei capsules improve gastrointestinal motility in rats with functional dyspepsia. J Tradit Chin Med 38(1):43–53. https://doi.org/10.1016/j.jtcm.2018.01.008
43. Barchetta I, Baroni MG, Melander O, Cavallo MG (2022) New insights in the control of fat homeostasis: the role of neurotensin. Int J Mol Sci 23(4):2209. https://doi.org/10.3390/ijms23042209
44. Gereau GB, Garrison SKD, McElligott ZA (2023) Neurotensin and energy balance. J Neurochem 166(2):189–200. https://doi.org/10.1111/jnc.15868
45. Wu Z, Stadler N, Abbaci A, Liu J, Boullier A, Marie N, Biondi O, Moldes M, Morichon R, Feve B, Melander O, Forgez P (2021) Effect of monoclonal antibody blockade of long fragment neurotensin on weight loss, behavior, and metabolic traits after high-fat diet induced obesity. Front Endocrinol 12:739287. https://doi.org/10.3389/fendo.2021.739287
46. Liguz-Lecznar M, Dobrzanski G, Kossut M (2022) Somatostatin and somatostatin-containing interneurons—from plasticity to pathology. Biomolecules 12(2):312. https://doi.org/10.3390/biom12020312
47. Shamsi BH, Chatoo M, Xu XK, Xu X, Chen XQ (2021) Versatile functions of somatostatin and somatostatin receptors in the gastrointestinal system. Front Endocrinol 12:652363. https://doi.org/10.3389/fendo.2021.652363
48. Fahrenkrug J (1979) Vasoactive intestinal polypeptide: measurement, distribution and putative neurotransmitter function. Digestion 19(3):146–169. https://doi.org/10.1159/000198339
49. Iwasaki M, Akiba Y, Kaunitz JD (2019) Recent advances in vasoactive intestinal peptide physiology and pathophysiology: focus on the gastrointestinal system. F1000Res 8:F1000. https://doi.org/10.12688/f1000research.18039.1
50. di Mario F, Cavallaro LG (2008) Non-invasive tests in gastric diseases. Dig Liver Dis 40(7):523–530. https://doi.org/10.1016/j.dld.2008.02.028
51. Rehfeld JF, Friis-Hansen L, Goetze JP, Hansen TVO (2007) The biology of cholecystokinin and gastrin peptides. Curr Top Med Chem 7(12):1154–1165
52. Ericsson P, Håkanson R, Rehfeld JF, Norlén P (2010) Gastrin release: antrum microdialysis reveals a complex neural control.

Regul Pept 161(1–3):22–32. https://doi.org/10.1016/j.regpep.2010.01.004
53. Helgadóttir H, Metz DC, Yang Y-X, Rhim AD, Björnsson ES (2014) The effects of long-term therapy with proton pump inhibitors on meal stimulated gastrin. Dig Liver Dis 46(2):125–130. https://doi.org/10.1016/j.dld.2013.09.021
54. Silman I (2021) The multiple biological roles of the cholinesterases. Prog Biophys Mol Biol 162:41–56. https://doi.org/10.1016/j.pbiomolbio.2020.12.001
55. Mori H, Verbeure W, Tanemoto R, Sosoranga ER, Jan T (2023) Physiological functions and potential clinical applications of motilin. Peptides 160:170905. https://doi.org/10.1016/j.peptides.2022.170905
56. Kitazawa T, Kaiya H (2021) Motilin comparative study: structure, distribution, receptors, and gastrointestinal motility. Front Endocrinol 12:700884. https://doi.org/10.3389/fendo.2021.700884
57. Li T, Yan Q, Wen Y, Liu J, Sun J, Jiang Z (2021) Synbiotic yogurt containing konjac mannan oligosaccharides and *Bifidobacterium animalis* ssp. *lactis* BB12 alleviates constipation in mice by modulating the stem cell factor (SCF)/c-kit pathway and gut microbiota. J Dairy Sci 104(5):5239–5255. https://doi.org/10.3168/jds.2020-19449
58. Sakata I, Takemi S (2021) Ghrelin-cell physiology and role in the gastrointestinal tract. Curr Opin Endocrinol Diabetes Obes 28(2):238–242. https://doi.org/10.1097/med.0000000000000610
59. Lennartsson J, Rönnstrand L (2012) Stem cell factor receptor/c-kit: from basic science to clinical implications. Physiol Rev 92(4):1619–1649. https://doi.org/10.1152/physrev.00046.2011
60. Chang YZG, Zhang YC, Liu YM, Fan MM (2023) Research progress in signaling pathways related to treatment of functional dyspepsia with traditional Chinese medicine. China J Chin Materia Med 48(20):5397–5403. https://doi.org/10.19540/j.cnki.cjcmm.20230619.601
61. Kitazawa T, Kaiya H (2019) Regulation of gastrointestinal motility by motilin and ghrelin in vertebrates. Front Endocrinol 10:278. https://doi.org/10.3389/fendo.2019.00278
62. Joung JY, Choi SH, Son CG (2021) Interstitial cells of Cajal: potential targets for functional dyspepsia treatment using medicinal natural products. Evid Based Complement Alternat Med 2021:9952691. https://doi.org/10.1155/2021/9952691
63. Liu Y, Yang L, Bi C, Tang K, Zhang B, Smaoui S (2021) *Nostoc sphaeroides* Kütz polysaccharide improved constipation and promoted intestinal motility in rats. Evid Based Complement Alternat Med 2021:1–11. https://doi.org/10.1155/2021/5596531
64. Kuang H, Zhang C, Zhang W, Cai H, Yang L, Yuan N, Yuan Y, Yang Y, Zuo C, Zhong F, Mariod A (2022) Electroacupuncture improves intestinal motility through exosomal miR-34c-5p targeting SCF/c-kit signaling pathway in slow transit constipation model rats. Evid Based Complement Alternat Med 2022:1–10. https://doi.org/10.1155/2022/8043841
65. Liu W, Zhi A (2021) The potential of quercetin to protect against loperamideinduced constipation in rats. Food Sci Nutr 9(6):3297–3307. https://doi.org/10.1002/fsn3.2296
66. Jin B, Ha SE, Wei L, Singh R, Zogg H, Clemmensen B, Heredia DJ, Gould TW, Sanders KM, Ro S (2021) Colonic motility is improved by the activation of 5-HT_{2B} receptors on interstitial cells of Cajal in diabetic mice. Gastroenterology 161(2):608-622.e7. https://doi.org/10.1053/j.gastro.2021.04.040
67. Yada T, Kohno D, Maejima Y, Sedbazar U, Arai T, Toriya M, Maekawa F, Kurita H, Niijima A, Yakabi K (2012) Neurohormones, rikkunshito and hypothalamic neurons interactively control appetite and anorexia. Curr Pharm Design 18(31):4854–4864. https://doi.org/10.2174/138161212803216898
68. Zhao Q, Xing F, Tao YY, Liu HL, Huang K, Peng Y, Feng NP, Liu CH (2020) Xiaozhang Tie improves intestinal motility in rats with cirrhotic ascites by regulating the stem cell factor/c-kit pathway in interstitial cells of Cajal. Front Pharmacol 11:1. https://doi.org/10.3389/fphar.2020.00001
69. Gong YY, Si XM, Lin L, Lu J (2012) Mechanisms of cholecystokinin-induced calcium mobilization in gastric antral interstitial cells of Cajal. World J Gastroenterol 18(48):7184–7193. https://doi.org/10.3748/wjg.v18.i48.7184
70. Hwang SJ, Wang JH, Lee JS, Lee HD, Choi TJ, Choi SH, Son CG (2021) Yeokwisan, a standardized herbal formula, enhances gastric emptying via modulation of the ghrelin pathway in a loperamide-induced functional dyspepsia mouse model. Front Pharmacol 12:753153. https://doi.org/10.3389/fphar.2021.753153
71. Zhang P (2022) Influence of foods and nutrition on the gut microbiome and implications for intestinal health. Int J Mol Sci 23(17):9588. https://doi.org/10.3390/ijms23179588
72. Hills R, Pontefract B, Mishcon H, Black C, Sutton S, Theberge C (2019) Gut microbiome: profound implications for diet and disease. Nutrients 11(7):1613. https://doi.org/10.3390/nu11071613
73. Wu Y, Wu Y, Wu H, Wu C, Ji E, Xu J, Zhang Y, Wei J, Zhao Y, Yang H (2021) Systematic survey of the alteration of the faecal microbiota in rats with gastrointestinal disorder and modulation by multicomponent drugs. Front Pharmacol 12:670335. https://doi.org/10.3389/fphar.2021.670335
74. Zhang J, Guo Z, Xue Z, Sun Z, Zhang M, Wang L, Wang G, Wang F, Xu J, Cao H, Xu H, Lv Q, Zhong Z, Chen Y, Qimuge S, Menghe B, Zheng Y, Zhao L, Chen W, Zhang H (2015) A phylo-functional core of gut microbiota in healthy young Chinese cohorts across lifestyles, geography and ethnicities. ISME J 9(9):1979–1990. https://doi.org/10.1038/ismej.2015.11
75. Zhang L, Liu C, Jiang Q, Yin Y (2021) Butyrate in energy metabolism: there is still more to learn. Trends Endocrinol Metab 32(3):159–169. https://doi.org/10.1016/j.tem.2020.12.003
76. Stoeva MK, Garcia-So J, Justice N, Myers J, Tyagi S, Nemchek M, McMurdie PJ, Kolterman O, Eid J (2021) Butyrate-producing human gut symbiont, *Clostridium butyricum*, and its role in health and disease. Gut Microbes 13(1):1–28. https://doi.org/10.1080/19490976.2021.1907272
77. Carretta MD, Quiroga J, López R, Hidalgo MA, Burgos RA (2021) Participation of short-chain fatty acids and their receptors in gut inflammation and colon cancer. Front Physiol 12:662739. https://doi.org/10.3389/fphys.2021.662739
78. Tang H, Zhan ZY, Zhang Y, Huang XX (2022) Propionylation of lysine, a new mechanism of short-chain fatty acids affecting bacterial virulence. Am J Transl Res 14(8):5773–5784
79. Yin Tong BL (2022) Research progress of physiological function of short-chain fatty acids in the intestine. Advances in Clinical Medicine 12(02):939–945. https://doi.org/10.12677/acm.2022.122137
80. Zhou L, Zeng Y, Zhang H, Ma Y (2022) The role of gastrointestinal microbiota in functional dyspepsia: a review. Front Physiol 13:910568. https://doi.org/10.3389/fphys.2022.910568
81. Andoh A, Tsujikawa T, Fujiyama Y (2003) Role of dietary fiber and short-chain fatty acids in the colon. Curr Pharm Design 9(4):347–358. https://doi.org/10.2174/1381612033391973
82. Parada Venegas D, De la Fuente MK, Landskron G, González MJ, Quera R, Dijkstra G, Harmsen HJM, Faber KN, Hermoso MA (2019) Short chain fatty acids (SCFAs)-mediated gut epithelial and immune regulation and its relevance for inflammatory bowel diseases. Front Immunol 10:277. https://doi.org/10.3389/fimmu.2019.00277